Inorganic Chemistry

ARTICLE

pubs.acs.org/IC

Crystal Structures of Au_2 Complex and Au_{25} Nanocluster and Mechanistic Insight into the Conversion of Polydisperse Nanoparticles into Monodisperse Au_{25} Nanoclusters

Huifeng Qian,[†,§] William T. Eckenhoff,[‡,§] Mark E. Bier,[†] Tomislav Pintauer,[*,‡] and Rongchao Jin[*,†]

[†]Department of Chemistry, Carnegie Mellon University, Pittsburgh, Pennsylvania 15213, United States

[‡]Department of Chemistry and Biochemistry, Duquesne University, Pittsburgh, Pennsylvania 15282, United States

Supporting Information

ABSTRACT: We previously reported a size-focusing conversion of polydisperse gold nanoparticles capped by phosphine into monodisperse $[Au_{25}(PPh_3)_{10}(SC_2H_4Ph)_5Cl_2]^{2+}$ nanoclusters in the presence of phenylethylthiol. Herein, we have determined the crystal structure of $[Au_{25}(PPh_3)_{10}(SC_2H_4Ph)_5Cl_2]^{2+}$ nanoclusters and also identified an important side-product—a Au(I) complex formed in the size focusing process. The $[Au_{25}(PPh_3)_{10}(SC_2H_4Ph)_5Cl_2]^{2+}$ cluster features a vertex-sharing bicosahedral core, resembling a rod. The formula of the Au(I) complex is determined to be $[Au_2(PPh_3)_2(SC_2H_4Ph)]^+$ by electrospray ionization (ESI) mass spectrometry, and its crystal structure (with SbF_6^- counterion) reveals Au−Au bridged by $-SC_2H_4Ph$ and with terminal bonds to two PPh_3 ligands. Unlike previously reported $[Au_2(PR_3)_2(SC_2H_4Ph)]^+$ complexes in the solid state, which exist as tetranuclear complexes (i.e., dimers of $[Au_2(PR_3)_2(SC_2H_4Ph)]^+$ units) through a Au···Au aurophilic interaction, in our case we found that the $[Au_2(PPh_3)_2(SC_2H_4Ph)]^+$ complex exists as a single entity, rather than being dimerized to form a tetranuclear complex. The observation of this Au(I) complex allows us to gain insight into the intriguing conversion process from polydisperse Au nanoparticles to monodisperse Au_{25} nanoclusters.

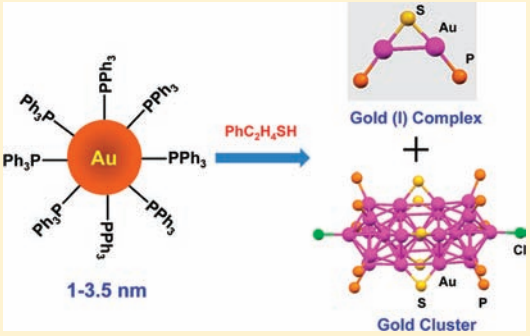

INTRODUCTION

Recent advances in the synthetic chemistry of ultrasmall gold nanoparticles (<2 nm) have rendered it possible to prepare atomically monodisperse nanoclusters protected by ligands.[1−10] These ultrasmall nanoparticles (or nanoclusters) exhibit interesting molecular-like optical properties (e.g., multiple absorption peaks and enhanced fluorescence),[11−16] charge transport properties,[17,18] intrinsic magnetism,[19] and so forth. A ubiquitous "size focusing" process has been observed in the synthetic processes, which permits the attainment of atomically monodisperse $Au_n(SR)_m$ nanoclusters via conversion from initially polydisperse nanoclusters.[2,20] Size conversion from well-defined starting clusters also allows one to produce new clusters.[5,10,14,21] In the gold−thiolate system, the gold(I)−thiolate complex constitutes the predominant side-product of the size evolution process; the Au(I)−SR complex can be easily separated from Au clusters due to its poor solubility in common solvents such as toluene and THF.[7b] Although some experimental and theoretical investigations have been performed,[22−27] the inability to effectively solubilize gold(I)−thiolate complexes makes it difficult to unravel their exact size (e.g., the number of Au−SR units in the complex) and atomic structures (e.g., ring or linear geometry).

In previous work, we reported the conversion of polydisperse Au nanoparticles (1−3.5 nm) to a monodisperse $[Au_{25}(PPh_3)_{10}(SR)_5Cl_2]^{2+}$ nanocluster via one-phase thiol etching.[20] Gold nanoparticles with a size larger than ∼2 nm possess a face-centered cubic (fcc) structure, whereas ultrasmall Au nanoparticles smaller than ∼2 nm often exhibit non-fcc structures.[28,29] A particularly interesting aspect in the conversion of 1−3.5 nm nanoparticles to $[Au_{25}(PPh_3)_{10}(SR)_5Cl_2]^{2+}$ nanoclusters is that the starting polydisperse Au nanoparticles are all converted to a specific-size cluster in the presence of thiol and triphenylphosphine.[20] The conversion process was not fully understood then, but one important factor should be due to the high stability of the final cluster, indicating that this is a thermodynamically driven process. Although the conversion of the nanoparticles in the presence of thiol ligands led to a single-sized nanocluster, it was not clear if other smaller side-products were formed simultaneously. The identification and structural characterization of the side-product(s) would offer important insights into the reaction mechanism.

In this work, we have identified an important byproduct in the conversion process from 1 to 3.5 nm nanoparticles to $[Au_{25}(PPh_3)_{10}(SR)_5Cl_2]^{2+}$ nanoclusters and successfully determined the crystal structures of both the gold(I) side-product and the $[Au_{25}(PPh_3)_{10}(SR)_5Cl_2]^{2+}$ nanocluster. These results have

Received: June 8, 2011
Published: October 11, 2011

helped our understanding of the size-focusing conversion process.

EXPERIMENTAL SECTION

Chemicals. Tetrachloroauric(III) acid ($HAuCl_4 \cdot 3H_2O$, 99.99%), 2-phenylethanethiol (99%), sodium borohydride ($NaBH_4$, 99.99%), toluene (HPLC grade, 99.9%), ethanol (HPLC grade), pentane (HPLC grade), chloroform (HPLC grade, 99.9%), and methanol (HPLC grade, 99%) were purchased from Sigma-Aldrich. Tetraoctylammonium bromide (TOAB, >98%) was obtained from Fluka. Triphenylphosphine (99%) was obtained from Acros Organics. Sodium hexafluoroantimonate(V) ($NaSbF_6$, 99.5%) was obtained from Alfa Aesar. All chemicals are used as received.

Preparation of Triphenylphosphine-Protected Au Nanoparticles. $HAuCl_4 \cdot 3H_2O$ (0.118 g, 0.3 mmol, dissolved in 5 mL H_2O) and TOAB (0.190 g, 0.348 mmol, dissolved in 10 mL toluene) were combined in a trineck round-bottom flask. Afterwards, the solution was vigorously stirred for ~15 min to effect phase transfer of Au(III) into toluene. The aqueous phase was then removed, and PPh_3 (0.9 mmol) was added to the toluene solution under vigorous stirring. The toluene solution became whitish cloudy. Then, $NaBH_4$ (0.034 g, 0.9 mmol, dissolved in 5 mL ethanol) was injected all at once. The solution immediately turned dark. The reaction was allowed to proceed for 2 hours under an air environment at room temperature. The crude black product (containing PPh_3-protected Au nanoparticles) was obtained after rotary evaporation of the solvent (toluene). The black product was washed several times with water and hexane to remove excess PPh_3 and TOAB. The product was further purified through precipitation by adding a mixed pentane/chloroform (6:1 vol) solvent to a solution of the nanoparticle product. The precipitated product was collected by centrifugation and then redissolved in methanol, followed by centrifugation again to remove insoluble components. The left solution of Au nanoparticles was dried by rotary evaporation, and the solids were collected for the subsequent experiments.

Conversion of Polydisperse Au Nanoparticles into Monodisperse Bi-icosahedral Au_{25} Nanoclusters. The bi-icosahedral $[Au_{25}(PPh_3)_{10}(SC_2H_4Ph)_5Cl_2]^{2+}$ clusters were synthesized by adding ~0.25 mL PhC_2H_4SH to a CH_2Cl_2 (20 mL) solution of phosphine-protected Au nanoparticles obtained in the above step (the ratio of PhC_2H_4SH/Au = 6:1). The solution was vigorously stirred for 12 h at room temperature. The products were obtained after drying the solution by rotary evaporation and washing with hexane and finally extraction with ethanol. The side-product $[Au_2(PPh_3)_2(SC_2H_4Ph)]^+$ coexists with $[Au_{25}(PPh_3)_{10}(SC_2H_4Ph)_5Cl_2]^{2+}$ clusters. The brownish yellow product was mixed with excess $NaSbF_6$ (~80 mg) for 15 min in CH_2Cl_2. Excess $NaSbF_6$ (white powder) was removed by centrifugation. The product was dried and redissolved in CH_2Cl_2/ethanol (1:1) for crystallization. After 1−2 days, crystals of two colors (orange and black) were obtained. The black crystals were determined to be $[Au_{25}(PPh_3)_{10}(SC_2Ph)_5Cl_2]^{2+}$, and the orange ones were $[Au_2(PPh_3)_2(SC_2H_4Ph)]^+$.

Characterization. UV−vis spectra of $[Au_2(PPh_3)_2(SC_2H_4Ph)]^+$ and $[Au_{25}(PPh_3)_{10}(SC_2H_4Ph)_5Cl_2]^{2+}$ (single crystals dissolved in CH_2Cl_2) were acquired on a Hewlett-Packard (HP) Agilent 8453 diode array spectrophotometer at room temperature. ESI-MS analysis was performed on a Waters Q-TOF II mass spectrometer and a Thermo-Fisher LCQ ESI/APCI ion trap mass spectrometer. The X-ray crystallographic data were collected at 150 K for $[Au_2(PPh_3)_2(SC_2H_4Ph)]^+SbF_6^-$ or at room temperature for $[Au_{25}(PPh_3)_{10}(SC_2H_4Ph)_5Cl_2]^{2+}(SbF_6^-)_2$ using graphite-monochromated Mo Kα radiation (0.71073 Å) with a Bruker Smart Apex II CCD diffractometer. Data reduction included absorption corrections with the multiscan method using SADABS. Structures were solved by Patterson methods and refined by full matrix least-squares using the SHELXTL 6.1 bundled software package. ORTEP-3 for Windows and Crystal Maker 7.2 were used to generate molecular graphics. Crystal data and experimental conditions are given in Supporting Information Tables S1 and S2.

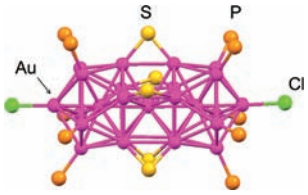

Figure 1. Structure of the $[Au_{25}(PPh_3)_{10}(SC_2H_4Ph)_5Cl_2]^{2+}$ cluster (color labels: Au, magenta; P, orange; S, yellow; Cl, green).

RESULTS AND DISCUSSION

We previously reported the size-focusing synthesis of gold clusters using 1−3.5 nm Au nanoparticles as the starting material.[20] The formula of the as-synthesized gold cluster was determined to be $[Au_{25}(PPh_3)_{10}(SC_2H_4Ph)_5Cl_2]^{2+}$ by ESI-mass spectrometry, thermogravimetric analysis (TGA), and nuclear magnetic resonance spectroscopy (NMR), but the crystal quality was too low for the structure to be solved.[20] Herein, we have been able to improve the crystal quality of $[Au_{25}(PPh_3)_{10}(SC_2H_4Ph)_5Cl_2]^{2+}$ clusters through crystallization in ethanol and CH_2Cl_2 (1:1, vol). The X-ray structure of the $[Au_{25}(PPh_3)_{10}(SC_2H_4Ph)_5Cl_2]^{2+}$ cluster is now solved (Figure 1), although the coordinating ligands are not fully resolved due to disordering. The Au_{25} core is composed of two icosahedral Au_{13} units by sharing one common vertex (i.e., $13 \times 2 - 1 = 25$ Au atoms), resembling a rod. Five thiolate ligands (only S atoms are shown) bridge the two icosahedrons, and 10 phosphines are terminally coordinated to the two Au_5 pentagonal rings on the two ends of the rod, and two chlorides bind to two apical Au atoms of the rod. The organic ligands (PPh_3 and PhC_2H_4S) could not be resolved through repeated attempts. It is noteworthy that the core framework of $[Au_{25}(PPh_3)_{10}(SC_2H_4Ph)_5Cl_2]^{2+}$ is identical to that of the ethylthiolate counterpart $[Au_{25}(PPh_3)_{10}(SC_2H_4)_5Cl_2]^{2+}$ reported by Tsukuda and co-workers previously.[5]

With respect to the conversion of polydisperse Au nanoparticles to $[Au_{25}(PPh_3)_{10}(SC_2H_4Ph)_5Cl_2]^{2+}$ clusters, some Au(I) complexes could be formed as byproducts in the course of the conversion process. Since two types of ligands are present in the solution (PPh_3 liberated from the starting nanoparticles and PhC_2H_4SH added in the size-focusing step), we speculate gold(I) complexes of several forms, such as $[Au(I)PPh_3]^+$, neutral $Au(I)SC_2H_4Ph$, and $Au(I)(PPh_3)(SC_2H_4Ph)$. We initially thought that certain $[Au(I)SC_2H_4Ph]_n$ complexes would most likely form due to stronger Au−S bonds than Au−P bonds, but herein we have indeed identified an interesting $[Au_2(PPh_3)_2(SC_2H_4Ph)]^+$ complex as a major byproduct formed in the size-focusing synthesis of $[Au_{25}(PPh_3)_{10}(SC_2H_4Ph)_5Cl_2]^{2+}$. Crystals of the $[Au_2(PPh_3)_2(SC_2H_4Ph)]^+$ complex was formed in the same solution of $[Au_{25}(PPh_3)_{10}(SC_2H_4Ph)_5Cl_2]^{2+}$ clusters in the crystallization experiment. Crystals of two colors (orange and black) were found. The black crystals are $[Au_{25}(PPh_3)_{10}(SC_2H_4Ph)_5Cl_2]^{2+}$. To determine the composition of the orange crystal, a single crystal was picked up and redissolved in methanol for an electrospray ionization mass spectrometry (ESI-MS) analysis. As shown in Figure 2, an intense peak at m/z 1055.14 was found, assigned as $[Au_2(PPh_3)_2(SC_2H_4Ph)]^+$ (calculated FW: 1055.16). Additionally, the isotope pattern

dx.doi.org/10.1021/ic2012292 |Inorg. Chem. 2011, 50, 10735–10739

Scheme 1. Proposed Mechanism for the Conversion of PPh_3-Protected Au Nanoparticles to Gold(I) Complex and $[Au_{25}(PPh_3)_{10}(SC_2H_4Ph)_5Cl_2]^{2+}$ Clusters

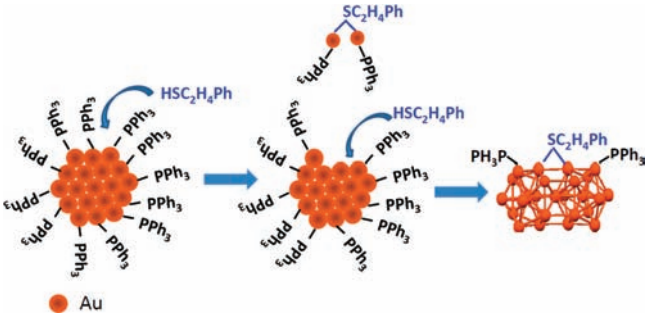

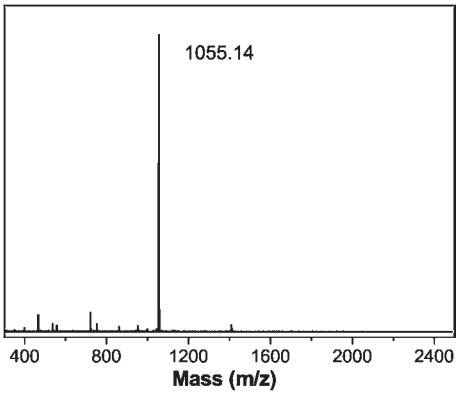

Figure 2. ESI mass spectrum of the gold(I) complex (positive mode).

shows a peak spacing of unity, indicating a singly charged species. It is interesting that this Au(I) complex unexpectedly contains both ligands of PPh_3 and -SC_2H_4Ph.

The structure of the orange crystals, $[Au_2(PPh_3)_2(SC_2H_4Ph)]^+[SbF_6^-]$, was further determined by X-ray crystallographic analysis (Figure 3). This complex contains two gold(I) centers with a roughly linear P−Au−S motif (angles: 174.5°). The two Au−P distances are 2.257 Å and 2.262 Å, which are typical of Au−P bonds. The two Au atoms are bridged by the thiolate ligand with Au−S distances of 2.318 and 2.329 Å and a Au−S−Au angle of 81.92°. The Au−Au distance of 3.046 Å is considerably shorter than the Au−Au distance in previously reported $[Au_2(PR_3)_2SR]^+$ dimers (3.10−3.20 Å),[30−33] indicating a stronger aurophilic attraction in our case.

It is noteworthy that many gold(I) complexes have been reported in the literature.[30−32] The previously reported gold complexes typically adopt a polynuclear structure through Au−Au aurophilic interactions originating from the relativistic London forces, with typical energies on the order of hydrogen bonds (5−15 kcal/mol).[31,32] Chen et al. reported a cationic $[Au_2(PR_3)_2SR]^+$ complex prepared by the oxidation of neutral mononuclear and dinuclear phosphine−gold(I)−thiolate complexes.[33] The cationic $[Au_2(PR_3)_2(SR)]^+$ complex existed as a dimer, i.e., a tetranuclear Au(I) structure with the four Au atoms arranged in a square planar geometry with pairs of gold atoms bridged by thiolate ligands. This structure could not be cleaved to give monomers of dinuclear species in solution.[33] In contrast, our work found that the $[Au_2(PPh_3)_2(SC_2H_4Ph)]^+$ complex exists only as a dinuclear Au(I) complex (as opposed to a dimer of the dinuclear complex) in both solution and solid states; no tetranuclear complexes were found in our analysis.

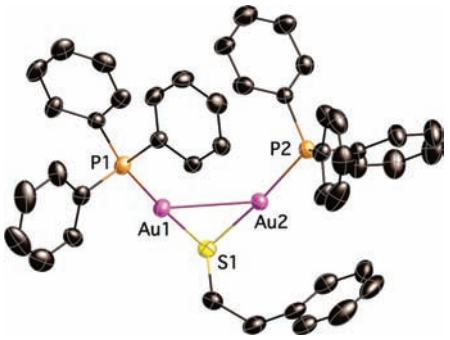

Figure 3. Structure of $[Au_2(PPh_3)_2(SC_2H_4Ph)]^+[SbF_6^-]$ shown with 30% probability ellipsoids. Selected distances (Å) and angles (deg) are Au(1)−Au(2), 3.046; Au(1)−P(1), 2.257; Au(1)−S(1), 2.318; Au(2)P(2), 2.262; Au(2)−S(1), 2.329; P(1)−Au(1)−S(1), 175.72; P(2)−A(2)−S(1), 173.40; Au(1)−S(1)−Au(2), 81.92°. Counterion: SbF_6. The X-ray data was collected at 150 K.

We further measured the UV−vis spectrum of the $[Au_2(PPh_3)_2(SC_2H_4R)]^+[SbF_6^-]$ complex (the orange crystals redissolved in CH_2Cl_2; Figure 4A). The absorption spectrum of this complex exhibits two bands at 268 and 275 nm as well as a weak, broad absorption tail extending from 280 nm to longer wavelengths, but no absorption is observed above 400 nm. This absorption spectrum is quite similar to that observed for diphosphine-bridged dinuclear Au(I) complex.[34−36] The absorption band could be assigned to the $d_{\sigma^*} \rightarrow p_\sigma$ transition, which is an indication of metal−metal interaction. The optical spectrum of the $[Au_2(PPh_3)_2(SC_2H_4Ph)]^+$ complex is completely different from that of the $[Au_{25}(PPh_3)_{10}(SC_2H_4Ph)_5Cl_2]^{2+}$ cluster (Figure 4B). The latter shows a distinct band at 670 nm and several additional bands at shorter wavelengths. The absorption at ~670 nm is assigned to a HOMO−LUMO electronic transition due to the dimeric structure, and those absorption peaks below 600 nm are assigned to the electronic transitions within individual icosahedral Au_{13} units.[37,38]

The identification and structural determination of the new gold(I) phosphine−thiolate complex offers important insight into the conversion of polydisperse Au nanoparticles into mondisperse $[Au_{25}(PPh_3)_{10}(SC_2H_4Ph)_5Cl_2]^{2+}$ clusters. Herein, we propose a mechanism for this process. The formation of $[Au_{25}(PPh_3)_{10}(SC_2H_4Ph)_5Cl_2]^{2+}$ and $[Au_2(PPh_3)_2(SC_2H_4Ph)]^+$ may be due to their high stability. The $[Au_{25}(SC_2H_4Ph)_5(PPh_3)_{10}Cl_2]^{2+}$ has 16 formal valence electrons, i.e., 25(Au 6s) − 5(thiolates) − 2(chloro) − 2(charges) = 16 e^-); note that PPh_3 is considered not to localize Au(6s) valence electrons and is hence not counted in. The 16 e^- count could be considered as a dimer of two 8 e^- units,[39] i.e., electron shell closing.[39,40] The bi-icosahedral 25-atom cluster is a quite ubiquitous structure, which has been observed in many phosphine-protected bimetal clusters (e.g., $Au_{13}Ag_{12}$, $Au_{12}Ag_{13}$) and trimetal clusters (e.g., $Au_{12}Ag_{12}Pt$, $Au_{11}Ag_{12}Pt_2$, $Au_{12}Ag_{12}Ni$).[41] Scheme 1 shows a plausible process for the size conversion from 1−3.5 nm nanoparticles to Au_{25} clusters. The surfaces of Au nanoparticles are initially stabilized by PPh_3 ligands; note that some Cl^- may also bind to nanoparticle surfaces. Excess PhC_2H_4SH reacts with Au nanoparticles due to strong interaction between thiol and gold. PhC_2H_4SH is expected to etch surface Au atoms and liberates them by releasing $[Au_2(PPh_3)_2(SC_2H_4Ph)]^+$. The partially bare nanoparticle surface would be further etched by thiols. With continuous etching, the gold particle size steadily decreases until the entire structure reorganizes to form the thermodynamically favored bi-icosahedral Au_{25} clusters.

dx.doi.org/10.1021/ic2012292 |Inorg. Chem. 2011, 50, 10735–10739

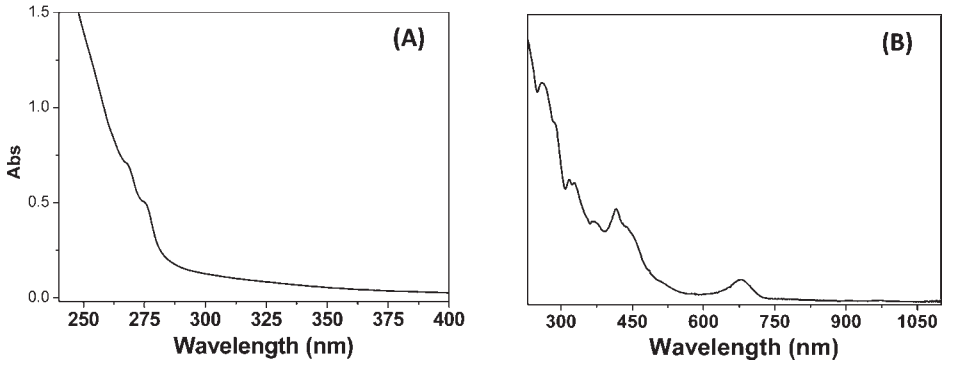

Figure 4. UV−vis spectra of $[Au_2(PPh_3)_2(SC_2H_4Ph)]^+$ (A) and $Au_{25}(PPh_3)_{10}(SC_2H_4Ph)_5Cl_2]^{2+}$ (B).

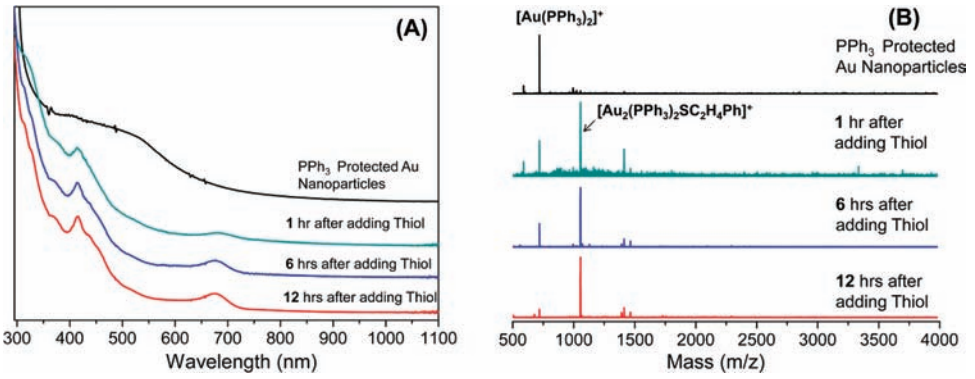

Figure 5. UV−vis (A) and ESI-MS (B) monitoring of the reaction process of thiol etching to PPh_3-protected Au nanoparticles. Crude samples were used in the optical and mass spectrometry analyses.

To further support the proposed mechanism, we have acquired time-dependent UV−vis spectra and ESI mass spectra during the thiol etching process (Figure 5). The evolution of the UV−vis spectra (Figure 5A) indicates the conversion from polydisperse PPh_3-protected Au nanoparticles to monodisperse $[Au_{25}(PPh_3)_{10}(SR)_5Cl_2]^{2+}$ nanoclusters. ESI mass spectra (Figure 5B) indicate that, prior to thiol etching, a $[Au(PPh_3)_2]^+$ complex (m/z 721.2) was observed, which is an impurity in the starting Au nanoparticles. After 1 h of thiol etching, we observed the dominant $[Au_2(PPh_3)_2(SC_2H_4Ph)]^+$ complex, together with minor $[Au(PPh_3)_2]^+$ and $[Au_3(PPh_3)_2(SC_2H_4Ph)_2]^+$ (m/z 1389.2) complexes (Figure 5B); of note, the accurate m/z values were determined in the 50−2,000 m/z detection mode, as the 50−4,000 m/z range in the turbo mode is less accurate for determining the m/z. Throughout the reaction (from 1 to 12 h), the $[Au_2(PPh_3)_2(SC_2H_4Ph)]^+$ complex remains a dominant byproduct; note that the $[Au_{25}(PPh_3)_{10}(SC_2H_4Ph)_5Cl_2]^{2+}$ cluster signal (m/z 4152)[20] is beyond the mass range in Figure 5B. Taken together, the proposed mechanism in which the thiol etching of Au nanoparticles occurs via the release of the $[Au_2(PPh_3)_2(SC_2H_4Ph)]^+$ complex should be at work.

CONCLUSION

In summary, we have identified a new gold(I) complex from the conversion of polydisperse Au nanoparticles to monodisperse $[Au_{25}(PPh_3)_{10}(SC_2H_4Ph)_5Cl_2]^{2+}$ clusters. The formula of the Au(I) complex has been determined to be $[Au_2(PPh_3)_2SC_2H_4Ph]^+$ by electrospray ionization (ESI) mass spectrometry. The crystal structures of both the Au(I) complex and the Au_{25} nanocluster have been determined. The $[Au_{25}(PPh_3)_{10}(SC_2H_4Ph)_5Cl_2]^{2+}$ cluster contains two icosahedral Au_{13} units by sharing one common vertex. In the $[Au_2(PPh_3)_2SC_2H_4Ph]^+$ complex, the two Au atoms form terminal bonds with two PPh_3's and are bridged by the thiolate ligand. Unlike other $[Au_2(PR_3)_2SR]^+$ complexes in solid states which exist as tetranuclear complexes (i.e., dimers of $Au_2(I)$ complexes) through Au···Au aurophilic interactions, the single unit of $[Au_2(PPh_3)_2SC_2H_4Ph]^+$ was observed in our work. The revealing of this gold(I) complex provides some important insight into the intriguing "size focusing" process and facilitates mechanistic understanding of the conversion process.

ASSOCIATED CONTENT

Supporting Information. CIF information for $[Au_{25}(PPh_3)_{10}(SC_2H_4Ph)_5Cl_2]^{2+}$ and $[Au_2(PPh_3)_2(SC_2H_4Ph)]^+$ (counterion: SbF_6^- in both cases). Crystal data and structure refinement for $[Au_{25}(PPh_3)_{10}(SR)_5Cl_2]^{2+}$ and $[Au_2(SC_2H_4Ph)(PPh_3)_2][SbF_6]$. This material is available free of charge via the Internet at http://pubs.acs.org.

AUTHOR INFORMATION

Corresponding Author

*E-mail: pintauert@duq.edu, rongchao@andrew.cmu.edu.

Author Contributions

§H.Q. and W. T. E. contributed equally to this work.

■ ACKNOWLEDGMENT

This material is partly based upon work supported by the Air Force Office of Scientific Research under AFOSR Award No. FA9550-11-1-9999 (FA9550-11-1-0147).

■ REFERENCES

(1) Jin, R. *Nanoscale* **2010**, *2*, 343−362 and references therein.
(2) Jin, R.; Qian, H.; Wu, Z.; Zhu, Y.; Zhu, M.; Mohanty, A.; Garg, N. *J. Phys. Chem. Lett.* **2010**, *1*, 2903–2910.
(3) Chaki, N. K.; Negishi, Y.; Tsunoyama, H.; Shichibu, Y.; Tsukuda, T. *J. Am. Chem. Soc.* **2008**, *130*, 8608–8610.
(4) Parker, J. F.; Fields-Zinna, C. A.; Murray, R. W. *Acc. Chem. Res.* **2010**, *43*, 1289–1296.
(5) Shichibu, Y.; Negishi, Y.; Watanabe, T.; Chaki, N. K.; Kawaguchi, H.; Tsukuda, T. *J. Phys. Chem. C* **2007**, *111*, 7845–7847.
(6) (a) Zhu, M.; Aikens, C. M.; Hollander, F. J.; Schatz, G. C.; Jin, R. *J. Am. Chem. Soc.* **2008**, *130*, 5883–5885. (b) Zhu, M.; Eckenhoff, W. T.; Pintauer, T.; Jin, R. *J. Phys. Chem. C* **2008**, *112*, 14221–14224.
(7) (a) Qian, H.; Eckenhoff, W. T.; Zhu, Y.; Pintauer, T.; Jin, R. *J. Am. Chem. Soc.* **2010**, *132*, 8280–8281. (b) Qian, H.; Zhu, M.; Andersen, U. N.; Jin, R. *J. Phys. Chem. A* **2009**, *113*, 4281–4284.
(8) Qian, H.; Jin, R. *Nano Lett.* **2009**, *9*, 4083–4087.
(9) Schaaff, T. G.; Knight, G.; Shafigullin, M. N.; Borkman, R. F.; Whetten, R. L. *J. Phys. Chem. B* **1998**, *102*, 10643–10646.
(10) (a) Pettibone, J. M.; Hudgens, J. W. *ACS Nano* **2011**, *5*, 2989–3002. (b) Pettibone, J. M.; Hudgens, J. W. *J. Phys. Chem. Lett.* **2010**, *1*, 2536–2540.
(11) Schaaff, T. G.; Whetten, R. L. *J. Phys. Chem. B* **2000**, *104*, 2630–2641.
(12) Muhammed, M. A. H.; Shaw, A. K.; Pal, S. K.; Pradeep, T. *J. Phys. Chem. C* **2008**, *112*, 14324–14330.
(13) Zheng, J.; Nicovich, P. R.; Dickson, R. M. *Annu. Rev. Phys. Chem.* **2007**, *58*, 409–431.
(14) Woehrle, G. H.; Hutchison, J. E. *Inorg. Chem.* **2005**, *44*, 6149–6158.
(15) Woehrle, G. H.; Brown, L. O.; Hutchison, J. E. *J. Am. Chem. Soc.* **2005**, *127*, 2172–2183.
(16) Jiang, D.-e.; Nobusada, K.; Luo, W.; Whetten, R. L. *ACS Nano* **2009**, *3*, 2351–2357.
(17) (a) Chen, S.; Murray, R. W. *Langmuir* **1999**, *15*, 682–689. (b) Wang, W.; Murray, R. W. *Langmuir* **2005**, *21*, 7015–7022. (c) Chen, W.; Chen, S. W. *Angew. Chem., Int. Ed.* **2009**, *48*, 4386–4389.
(18) (a) Toikkanen, O.; Carlsson, S.; Dass, A.; Rnnholm, G.; Kalkkinen, N.; Quinn, B. M. *J. Phys. Chem. Lett.* **2010**, *1*, 32–37. (b) Laaksonen, T.; Ruiz, V.; Liljeroth, P.; Quinn, B. M. *Chem. Soc. Rev.* **2008**, *37*, 1836–1846.
(19) Zhu, M.; Aikens, C. M.; Hendrich, M. P.; Gupta, R.; Qian, H.; Schatz, G. C.; Jin, R. *J. Am. Chem. Soc.* **2009**, *131*, 2490–2492.
(20) Qian, H.; Zhu, M.; Lanni, E.; Zhu, Y.; Bier, M. E.; Jin, R. *J. Phys. Chem. C* **2009**, *113*, 17599–17603.
(21) Nimmala, P. R.; Dass, A. *J. Am. Chem. Soc.* **2011**, *133*, 9175–9177.
(22) Shaw, C. F. *Chem. Rev.* **1999**, *99*, 2589–2600.
(23) Sun, Q.-F.; Lee, T. K.-M.; Li, P.-Z.; Yao, L.-Y.; Huang, J.-J.; Huang, J.; Yu, S.-Y.; Li, Y.-Z.; Cheng, E. C.-C.; Yam, V. W.-W. *Chem. Commun.* **2008**, 5514–5516.
(24) (a) Kacprzak, K. A.; Lopez-Acevedo, O.; Hakkinen, H.; Gronbeck, H. *J. Phys. Chem. C* **2010**, *114*, 13571–13576. (b) Barngrover, B. M.; Aikens, C. M. *J. Phys. Chem. Lett.* **2011**, 990–994.
(25) Simpson, C. A.; Farrow, C. L.; Tian, P.; Billinge, S. J. L.; Huffman, B. J.; Harkness, K. M.; Cliffel, D. E. *Inorg. Chem.* **2011**, *49*, 10858–10866.
(26) Shao, N.; Pei, Y.; Gao, Y.; Zeng, X. C. *J. Phys. Chem. A* **2009**, *113*, 629–632.
(27) Tang, Z.; Xu, B.; Wu, B.; Germann, M. W.; Wang, G. *J. Am. Chem. Soc.* **2010**, *132*, 3367–3374.
(28) Jin, R.; Zhu, Y.; Qian, H. *Chem.—Eur. J.* **2011**, *17*, 6584–6593.
(29) Wu, Z.; Chen, J.; Jin, R. *Adv. Func. Mater.* **2011**, *21*, 177–183.
(30) Schmidbaur, H. *Gold Bull.* **1990**, *23*, 11–20.
(31) Hunks, W. J.; Jennings, M. C.; Puddephatt, R. J. *Inorg. Chem.* **2000**, *39*, 2699–2702.
(32) Balzano, F.; Cuzzola, A.; Diversi, P.; Ghiotto, F.; Uccello-Barretta, G. *Eur. J. Inorg. Chem.* **2007**, 5556–5562.
(33) Chen, J.; Jiang, T.; Wei, G.; Mohamed, A. A.; Homrighausen, C.; Krause Bauer, J. A.; Bruce, A. E.; Bruce, M. R. M. *J. Am. Chem. Soc.* **1999**, *121*, 9225–9226.
(34) Jaw, H. R. C.; Savas, M. M.; Rogers, R. D.; Mason, W. R. *Inorg. Chem.* **1989**, *28*, 1028–1037.
(35) Leung, K. H.; Phillips, D. L.; Mao, Z.; Che, C.-M.; Miskowski, V. M.; Chan, C.-K. *Inorg. Chem.* **2002**, *41*, 2054–2059.
(36) Brinas, R. P.; Hu, M.; Qian, L.; Lymar, E. S.; Hainfeld, J. F. *J. Am. Chem. Soc.* **2007**, *130*, 975–982.
(37) Nobusada, K.; Iwasa, T. *J. Phys. Chem. C* **2007**, *111*, 14279–14282.
(38) Sfeir, M. Y.; Qian, H.; Nobusada, K.; Jin, R. *J. Phys. Chem. C* **2011**, *115*, 6200–6207.
(39) Walter, M.; Akola, J.; Lopez-Acevedo, O.; Jadzinsky, P. D.; Calero, G.; Ackerson, C. J.; Whetten, R. L.; Gronbeck, H.; Hakkinen, H. *Proc. Natl. Acad. Sci. U.S.A.* **2008**, *105*, 9157–9162.
(40) Jiang, D.-E.; Dai, S. *Inorg. Chem.* **2009**, *48*, 2720–2722.
(41) Teo, B. K.; Zhang, H. *Coord. Chem. Rev.* **1995**, *143*, 611–636.